Letter to the Editor

The impacts of time of echo (TE) and time of repetition (TR) on diffusion-derived 'vessel density' (DDVD) measurement: examples of liver, spleen, and hepatocellular carcinoma

Yì Xiáng J. Wáng^, Cai-Ying Li, Dian-Qi Yao, Sheng-Nan Tang, Ben-Heng Xiao

Department of Imaging and Interventional Radiology, Faculty of Medicine, The Chinese University of Hong Kong, Shatin, New Territories, Hong Kong SAR, China

Correspondence to: Yì Xiáng J. Wáng, PhD. Department of Imaging and Interventional Radiology, Faculty of Medicine, The Chinese University of Hong Kong, 30-32 Ngan Shing Street, Shatin, New Territories, Hong Kong SAR, China. Email: yixiang_wang@cuhk.edu.hk.

Submitted Feb 05, 2025. Accepted for publication Mar 10, 2025. Published online Mar 13, 2025.
doi: 10.21037/qims-2025-270
View this article at: https://dx.doi.org/10.21037/qims-2025-270

Studies on liver diffusion-weighted imaging (DWI) revealed that diffusion-derived 'vessel density' (DDVD) can reflect microvascular perfusion. Liver blood vessels including sub-pixel microvessels show high signal when there is no motion probing gradient (b=0 s/mm^2) and low signal when even very low b-values (such as b=1, b=2 s/mm^2) are applied (1). Thus, the signal difference between images when the motion probing gradient is 'off' and 'on' reflects the extent of tissue vessel density in the physiological sense, and we term this 'DDVD'. DDVD is derived from the equation (1,2):

$$DDVD(b_0,b_2)=\frac{Sb_0}{ROIarea_0}-\frac{Sb_2}{ROIarea_2};\left[unit:\frac{arbitrary\ unit\,(au)}{pixel}\right] \quad [1]$$

where $ROIarea_0$ and $ROIarea_2$ refer to the number of pixels in the selected region of interest (ROI) on b=0 and b=2 s/mm^2 DWI, respectively. Sb_0 refers to the measured sum signal intensity within the ROI when b=0 s/mm^2, and Sb_2 refers to the measured sum signal intensity within the ROI when b=2 s/mm^2, thus $Sb/ROIarea$ equates to the mean signal intensity within the ROI. Sb_2 and $ROIarea_2$ can also be approximated by other low b-values DWI. As absolute magnetic resonance (MR) signal intensity is influenced by various factors, including B0/B1 spatial inhomogeneity, coil loading, receiver gain, etc., the ratio of a lesion to its adjacent native tissue (such as the $DDVD_{HCC}/DDVD_{liver}$ ratio, HCC: hepatocellular carcinoma) can be used to minimize these scaling factors. DDVD measure based on this simple principle is useful as a straightforward imaging biomarker in diverse clinical scenarios (2-14).

For DWI, a long time of repetition (TR) and a modest time of echo (TE) are commonly used for data acquisition. A long TR is useful to minimize the 'T1 effect' [which is defined as magnetic resonance imaging (MRI) signal differences contributed by T1 relaxation time difference]. In our liver DWI and intravoxel incoherent motion (IVIM) studies, TE of around 60 ms has been applied. We have recently demonstrated that, for liver and spleen DDVD measurement, when the 2nd b-value is 1 or 2 s/mm^2, and the TE is 63 ms (TR: 1,600 ms), $DDVD_{liver}$ is approximately similar to $DDVD_{spleen}$ which agrees with the known physiology that liver and spleen have similar amounts of blood perfusion (13). According to the analysis in (13), DDVD value of 11 arbitrary unit (au)/pixel at 1.5 T or 35 au/pixel at 3.0 T will be approximately equivalent to computed tomography (CT) perfusion of blood volume of 18 mL/100 mL with a blood flood speed of around 1.2 mL/min/mL (*Figure 1A*,*1B*). This also correlates to the liver IVIM-perfusion fraction (IVIM-PF) measure of about 18% reported by us (15). In physiological studies, the hepatic blood volume including that of the large vessels is about 25 mL/100 g and blood flow is about 1.04 mL/min/mL (16).

^ ORCID: 0000-0001-5697-0717.

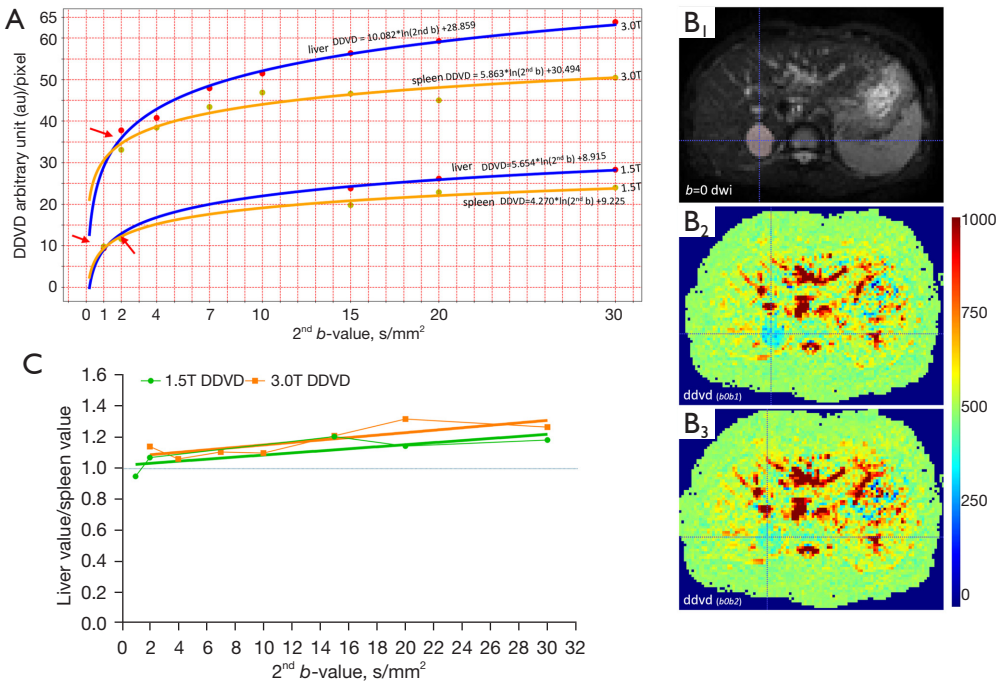

Figure 1 Liver DDVD and spleen DDVD comparison with healthy volunteer studies. (A) 1.5 T scan had 26 subjects and 3.0 T scan had 19 subjects. 1.5 T scan had TR of 1,600 ms (acquired with respiratory gating) and TE of 63 ms, and 3.0 T scan had TR of 1,600 ms and TE of 59 ms (acquired with free breathing). For liver and spleen DDVD measurement, when the 2nd *b*-value is 1 or 2 mm^2/s, $DDVD_{liver}$ is approximately similar to $DDVD_{spleen}$ (arrows in A). (B) While spleen shows a higher signal on DWI *b*=0 mm^2/s image (B1), on the maps of $DDVD_{b0b1}$ (B2) and $DDVD_{b0b2}$ (B3), liver signal and spleen signal appear similiar (1.5 T data). (C) An increasing 2nd *b*-value is associated with a slowly increasing $DDVD_{liver}/DDVD_{spleen}$ ratio, and this is slightly more apparent with 3.0 T data. Since when 2nd *b*-value is >2 s/mm^2, DDVD mainly reflects blood volume, results in (C) is consistent with the fact that liver has a slightly higher blood volume as shown with perfusion CT and nuclear medicine studies (13). Data of this graph is based on (13). DDVD, diffusion-derived 'vessel density'; TE, time of echo; TR, time of repetition.

As *in vivo* diffusion metrics can be only measured with MRI thus external validation is not possible for diffusion metrics (17), it will be convenient and practical for us to consider liver/spleen parenchyma as the reference tissues. Our modeling analysis shows that, when the 2nd *b*-value is very low (such as 1 or 2 s/mm^2), liver DDVD is contributed by both blood pool volume and blood flow speed; however, when the 2nd *b*-value is only low (such as 10 or 20 s/mm^2), then liver DDVD is more contributed by blood pool volume (3). In fact, the blood pool volume of the liver is slightly larger than that of the spleen, while the blood flow speed of the spleen is slightly faster than that of the liver [see *Tab. 1* and *Tab. 2* in (13)]. Moreover, a shorter T2 relaxation time (T2) of the liver than that of the spleen (liver T2: 40 ms, spleen T2: 60 ms, 3.0 T data) leads to a faster signal decay during DWI signal acquisition and promotes fast compartment measurement (18-20). T2 values are shorter at 3.0 T than at 1.5 T. These factors likely promote the $DDVD_{liver}$ value over $DDVD_{spleen}$ value when the 2nd *b*-value is increasingly larger till the 2nd *b*-value is 30 s/mm^2, and also promote the difference between $DDVD_{liver}$ and $DDVD_{spleen}$ being greater at 3.0 T than at 1.5 T (*Figure 1C*). Note that, an application of the diffusion gradients will lead to a decrease in observed T2 for tissues which can be interpreted as an application of diffusion gradients is associated with a longer TE for data acquisition (21), and it is likely that that a stronger diffusion gradient (i.e., a higher *b*-value) will lead to an even shorter observed T2. *Figure 1C* shows, an increasing 2nd *b*-value is associated with a slowly increasing $DDVD_{liver}/DDVDs_{pleen}$ ratio, and this is slightly more apparent with 3.0 T data. Such a trend is interpreted as a 'T2 effect' which is contributed by the T2 relaxation time difference. When the 2nd *b*-value is ≤20 s/mm^2, $DDVD_{liver}/DDVDs_{pleen}$ ratio can reach up to 1.25; this

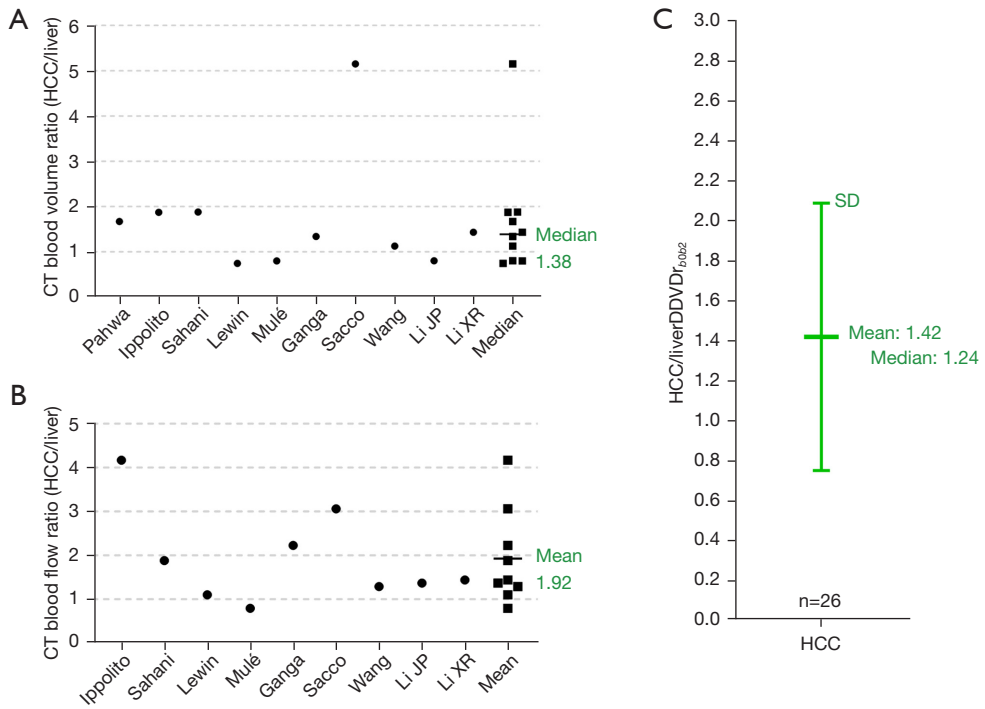

Figure 2 HCC measure to surround liver parenchyma measure ratios of perfusion CT measured blood volume (A), blood flow speed (B), and DDVD (C). The $DDVD_{HCC}/DDVD_{liver}$ ratio agrees well with the HCC/liver ratio of perfusion CT measured blood volume. (A) and (B) are the based on a random selection of the reports of Pahwa *et al.* (22), Ippolito *et al.* (23), Sahani *et al.* (24), Lewin *et al.* (25), Mulé *et al.* (26), Ganga *et al.* (27), Sacco *et al.* (28), Wang *et al.* (29), Li JP *et al.* (30), Li XR *et al.* (31). (C) is based on the authors' own data of 26 cases of HCC. DDVDr was measured at 3.0 T, with a TE of 59 ms (TR: 1,600 ms, acquired with free breathing) and b=0, 2 s/mm^2. CT, computed tomography; DDVD, diffusion-derived 'vessel density'; DDVDr, DDVD ratio; HCC, hepatocellular carcinoma; SD, standard deviation; TE, time of echo; TR, time of repetition.

remains reasonable since liver blood pool volume is indeed slightly larger than that of the spleen. When a TE of 59 ms (TR: 1,600 ms) and b=0, 2 s/mm^2 were used for DDVD calculation of 26 cases of HCC, we measured a mean $DDVD_{HCC}/DDVD_{liver}$ ratio of 1.42. This value agrees well with perfusion CT blood volume literature results median ratio of 1.38, while perfusion CT blood flow literature results mean ratio is 1.92 [*Figure 2* (22-31)]. Moreover, in a recent study of parotid tumors (14), we used DDVD ratio (DDVDr, TR =2,000 ms, TE =50 ms) to evaluate 24 pleomorphic adenomas (PA), 14 malignant tumors, and 16 Warthin's tumors. DDVDr was DDVD of the tumor divided by DDVD of tumor free parotid gland tissue. A literature search was conducted for parotid gland tumor perfusion CT studies. Perfusion parameters of PAs, malignant tumors, and Warthin's tumors were further normalized by the PA measure (thus the normalized measure for PA is 1). The ratio results of malignant tumor DDVD and Warthin's tumors DDVD were compared with literature results. It was noted that DDVDr ratios of both *malignant tumor to PA* (1.56) and *Warthin's tumor to PA* (2.47) were very similar to the literature data mean ratio of CT measured blood volume of these tumors (1.54 for *malignant tumor to PA*, and 2.51 for *Warthin's tumor to PA*).

However, our recent observations show both a long TE or a short TR can depress the DDVD measure for a tissue with a shorter T2/shorter T1 in relative terms. *Figure 3* shows $DDVD_{spleen}/DDVD_{liver}$ ratio for 12 cases of focal nodular hyperplasia (FNH) and liver metastasis patients and 7 cases of HCC patients. When TE was 84 ms (TR =2,500 ms), $DDVD_{spleen}$ was measured higher than $DDVD_{liver}$. As HCC patients were more likely to have liver fibrosis background, thus $DDVD_{spleen}/DDVD_{liver}$ was even higher for HCC patients than patients with FNH or with liver metastasis. When TR is shortened, $DDVD_{spleen}/DDVD_{liver}$ ratio is also promoted (*Figure 4A*).

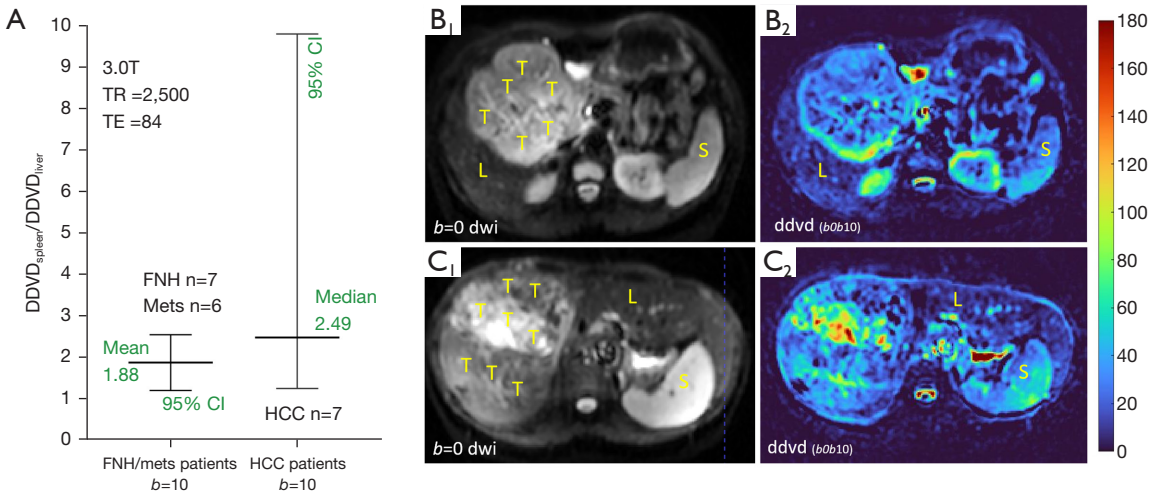

Figure 3 $DDVD_{spleen}/DDVD_{liver}$ ratio for data acquired with TE being 84 ms (TR =2,500 ms, acquired with respiratory gating) and 2nd *b*-value being 10 s/mm^2. (A) Non-tumor regions of the liver were measured. (B,C) Two cases' DDVD maps calculated with *b*=0 and *b*=10 s/mm^2 DWI images, with spleen (S) showing higher signal than liver (L). T denotes the tumor regions. Unit for TR and TE is millisecond. CI, confidence interval; DDVD, diffusion-derived 'vessel density'; DWI, diffusion-weighted imaging; FNH, focal nodular hyperplasia; HCC, hepatocellular carcinoma; Mets, metastasis; TE, time of echo; TR, time of repetition.

When a TR of 313 ms (TE =38 ms) was applied for data acquisition, another set of 3.0 T DWI data of ours shows $DDVD_{spleen}/DDVD_{liver}$ ratio was 3.75 when the 2nd *b*-value was 2 s/mm^2, and 2.69 when the 2nd *b*-value was 10 s/mm^2 (*Figure 4B,4C*). However, shortening of TE from 60 to 46 ms does not appear to have a substantial impact on $DDVD_{spleen}/DDVD_{liver}$ ratio. Because the spleen has different T1/T2 compared to the liver (liver of 810 ms and spleen of 1,330 ms for T1, liver of 40 ms and spleen of 60 ms for T2, 3.0 T measures), the analyses above demonstrate that, depending on the TR/TE, $DDVD_{spleen}$ can be measured higher or slightly lower relative to $DDVD_{liver}$. Therefore, only with the right combination of TR/TE and *b*-values, $DDVD_{spleen}$ can be measured similar to $DDVD_{liver}$. This is further supported by our analyses of HCC DDVD results as discussed below.

When TE of 84 ms and TR of 2,500 ms were used to acquire DWI, with one dataset we measured a mean $DDVD_{HCC}/DDVD_{liver}$ ratio of 5.807 (2nd *b*-value =10 s/mm^2, *Figure 5A*). When TR of 313 ms (TE =38 ms) was used to acquire liver DWI data, with one dataset we measured a mean $DDVD_{HCC}/DDVD_{liver}$ ratio of 2.702 (2nd *b*-value =10 s/mm^2, *Figure 5B*). These results are consistent with the $DDVD_{spleen}/DDVD_{liver}$ ratio results noted above. Fortunately, the moderate TE of around 60 ms is the most commonly used echo time in practice, and a long TR is commonly applied to minimize the T1 effect and allow better longitudinal spin recovery to improve the signal. On the other hand, as demonstrated in *Figure 5*, a shorter TR or longer TE can be implemented to further enhance lesion to liver contrast ratio on DDVD map. However, longer TE and shorter TR are associated with lower signal-to-noise ratio. In the meantime, short TR can be applied to speed up data acquisition, allowing breathhold imaging.

TE's impact on the diffusion metric of ADC has been noted (20), as well as its impact on IVIM measures (18,19,32,33). In the study of 5 healthy volunteers' liver reported by Jerome *et al.* (32), IVIM-PF was measured to be 22.4%, 24.4%, 26.4%, 28.5%, and 30.7%, respectively, for TE of 62, 72, 82, 92, and 102 ms. In our systematic review, it was noted that liver IVIM-PF was on average 22% (34). With our own liver and spleen IVIM-PF qualification, the IVIM protocol had a *b*-value distribution of 0, 2, 4, 7, 10, 15, 20, 30, 46, 60, 72, 100, 150, 200, 400, and 600 s/mm^2. The data were acquired with a 1.5 T scanner with TR of 1,600 ms and TE of 63 ms, and the curve fitting was based on bi-exponential segmented fitting (starting from *b* =0 s/mm^2 data and with threshold *b*-value of 60 s/mm^2). We have measured liver IVIM-PF to be 18% (15). This approximately agrees with perfusion CT and physiological measurement results (13,16). However, we measured spleen IVIM-PF being 9% which was highly underestimated (15). Though the blood flow speed is slightly higher in spleen than in liver [reviewed in (13)], IVIM-D_{fast} was also

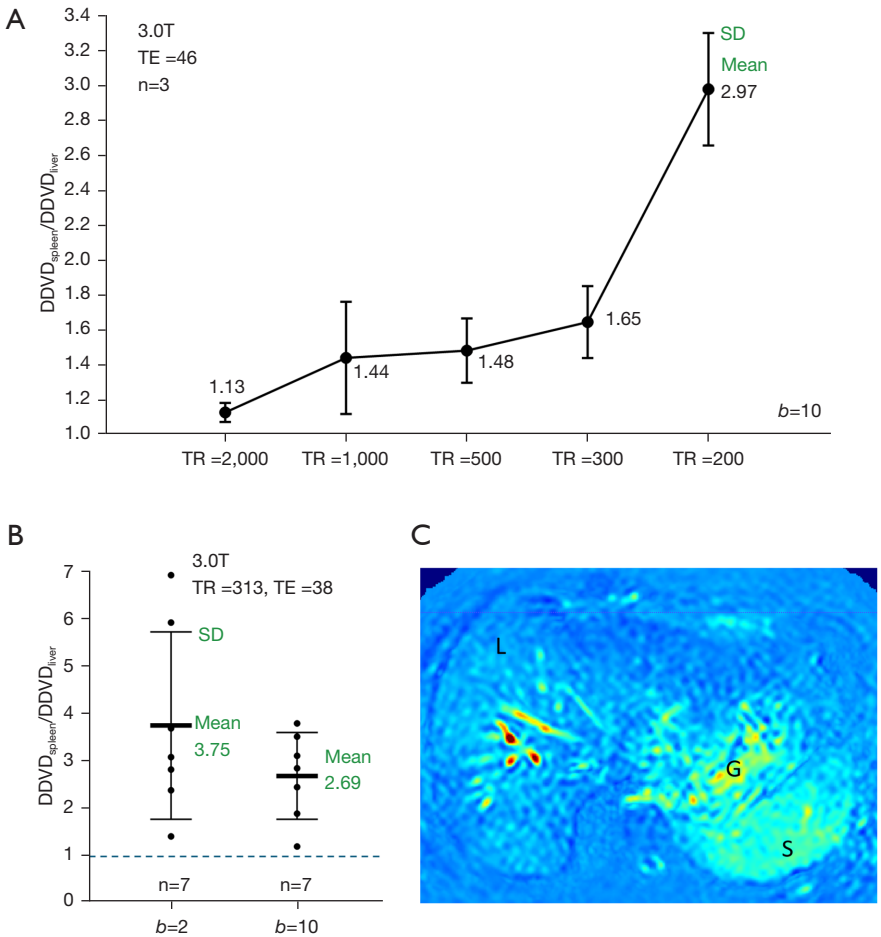

Figure 4 Impact of TR on DDVD$_{spleen}$/DDVD$_{liver}$ ratio. (A) The measures of (only) three heathy volunteers (mean and SD). When TR is 2,000 ms and TE is 46 ms (acquired with free breathing), DDVD$_{spleen}$/DDVD$_{liver}$ ratio is 1.13 thus being approximately consistent with results in *Figure 1* and also showing shortening of TE has no substantial impact on DDVD$_{spleen}$/DDVD$_{liver}$ ratio. Shortening of TR to 1,000, to 500, to 300, and to 200 ms is associated with an increase of DDVD$_{spleen}$/DDVD$_{liver}$ ratio. (B) DDVD$_{spleen}$/DDVD$_{liver}$ ratio of seven HCC cases (acquired with breathhold). Non-tumor regions of the liver were measured. Three cases did not have liver fibrosis, and four cases had grade-1 liver fibrosis. DDVD$_{spleen}$/DDVD$_{liver}$ ratio is presented with scatter plot and mean/SD. It is noted that for all seven cases, DDVD$_{spleen}$ is measured higher than DDVD$_{liver}$. DDVD$_{spleen}$/DDVD$_{liver}$ ratio is higher when the 2nd *b*-value is 2 s/mm^2 than the 2nd *b*-value is 10 s/mm^2. (C) An example DDVD map calculated with *b*=0 and *b*=2 s/mm^2 DWI images [case from (B)], with spleen (S) showing higher signal than liver (L). Unit for TR and TE is millisecond. DDVD, diffusion-derived 'vessel density'; G, gastric fluid; HCC, hepatocellular carcinoma; SD, standard deviation; TE, time of echo; TR, time of repetition.

measured markedly lower in spleen than in liver (15). For spleen IVIM-PF to be measured around 18%, TE should be extended longer to compensate for the longer T2 of spleen (20). IVIM analysis also underestimates the IVIM-PF of HCC due to its longer T2 relative to the T2 of liver parenchyma (33). Accordingly, for the quantification of HCC IVIM-PF, a TE longer than 60 ms is needed as the mean T2 of HCC is around 60 ms. When TE is around 60 ms as the case for most abdominal DWI, ADC$_{spleen}$ is also underestimated. For example, using TE of 66 ms (TR: 8,750 ms) and two *b*-values of 0 and 800 s/mm^2, Kim *et al.* (35) reported ADC$_{liver}$ of 1.07×10^{-3} mm^2/s and ADC$_{spleen}$ of 0.79×10^{-3} mm^2/s. Compared with the liver, the spleen has a higher water content [with longer T1/T2, higher free water content (36), and lower density on CT image (37)], it is more reasonable that the spleen has higher true tissue diffusion (own unpublished data).

One of the initial goals of using DDVD was to minimize

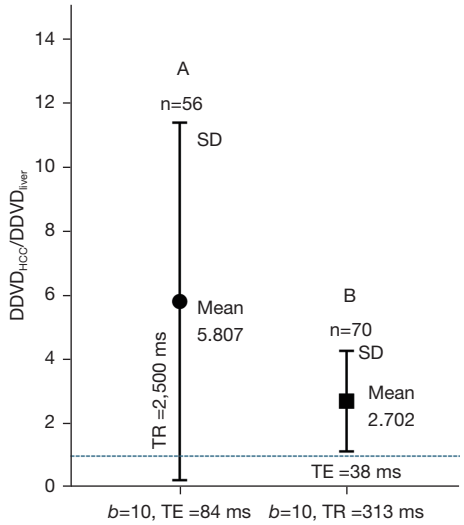

Figure 5 Compared with the cases of a long TR and a short/moderate TE (see *Figures 2,4* results), both the applications of a long TE of 84 or a short TR of 313 lead to a higher DDVD$_{HCC}$/DDVD$_{liver}$ ratio. Data A had 56 cases of HCC, and image data acquisition at 3.0 T had TR of 2,500 ms (acquired with respiratory gating) and TE of 84 ms. Data B had 70 cases of HCC, and image data acquisition at 3.0 T had TR of 313 ms (acquired with breathhold) and TE of 38 ms. The 2nd *b*-value for DDVD is both 10 s/mm^2 for the data in this graph. Unit for TR and TE is millisecond. DDVD, diffusion-derived 'vessel density'; HCC, hepatocellular carcinoma; SD, standard deviation; TE, time of echo; TR, time of repetition.

the 'T2 effect'. This is approximately achieved when TR is long, TE is short or modest, and the 2nd *b*-value is very low, as shown in our analyses for the relative blood volume of the liver, spleen, and HCC (*Figures 1,2*). DDVD is less sensitive to TE selection and 'T2 effect' compared to those of IVIM and ADC (13,18,19,32,33,38,39).

Acknowledgments

Parts of the research was conducted at the Chinese University of Hong Kong (CUHK) MRI Facility, which is jointly funded by Kai Chong Tong, HKSAR Research Matching Grant Scheme and the Department of Imaging and Interventional Radiology, The CUHK.

Footnote

Funding: None.

Conflicts of Interest: All authors have completed the ICMJE uniform disclosure form (available at https://qims.amegroups.com/article/view/10.21037/qims-2025-270/coif). Y.X.J.W. serves as the Editor-in-Chief of *Quantitative Imaging in Medicine and Surgery*. Y.X.J.W. is the founder of Yingran Medicals Ltd., which develops medical image-based diagnostics software. B.H.X. contributed to the development of Yingran Medicals Ltd. The other authors have no conflicts of interest to declare.

Ethical Statement: The authors are accountable for all aspects of the work in ensuring that questions related to the accuracy or integrity of any part of the work are appropriately investigated and resolved.

References

1. Wáng YXJ. Living tissue intravoxel incoherent motion (IVIM) diffusion MR analysis without b=0 image: an example for liver fibrosis evaluation. Quant Imaging Med Surg 2019;9:127-33.
2. Xiao BH, Huang H, Wang LF, Qiu SW, Guo SW, Wáng YXJ. Diffusion MRI Derived per Area Vessel Density as a Surrogate Biomarker for Detecting Viral Hepatitis B-Induced Liver Fibrosis: A Proof-of-Concept Study. SLAS Technol 2020;25:474-83.
3. Ma FZ, Xiao BH, Wáng YXJ. MRI signal simulation of liver DDVD (diffusion derived 'vessel density') with multiple compartments diffusion model. Quant Imaging Med Surg 2025;15:1710-8.
4. He J, Chen C, Xu L, Xiao B, Chen Z, Wen T, Wáng YXJ, Liu P. Diffusion-Derived Vessel Density Computed From a Simplified Intravoxel Incoherent Motion Imaging Protocol in Pregnancies Complicated by Early Preeclampsia: A Novel Biomarker of Placental Dysfunction. Hypertension 2023;80:1658-67.
5. Li CY, Chen L, Ma FZ, Chen JQ, Zhan YF, Wáng YXJ.

High performance of the diffusion magnetic resonance imaging biomarker diffusion-derived 'vessel density' (DDVD) for separating placentas associated with pre-eclampsia from placentas in normal pregnancy. Quant Imaging Med Surg 2025;15:1-14.
6. Lu T, Wang L, Li M, Wang Y, Chen M, Xiao BH, Wáng YXJ. Diffusion-derived vessel density (DDVD) computed from a simple diffusion MRI protocol as a biomarker of placental blood circulation in patients with placenta accreta spectrum disorders: A proof-of-concept study. Magn Reson Imaging 2024;109:180-6.
7. Hu GW, Li CY, Zhang G, Zheng CJ, Ma FZ, Quan XY, Chen W, Sabarudin A, Zhu MSY, Li XM, Wáng YXJ. Diagnosis of liver hemangioma using magnetic resonance diffusion-derived vessel density (DDVD) pixelwise map: a preliminary descriptive study. Quant Imaging Med Surg 2024;14:8064-82.
8. Chen JQ, Li CY, Wang W, Yao DQ, Jiang RF, Wáng YXJ. Diffusion-derived vessel density (DDVD) for penumbra delineation in brain acute ischemic stroke: initial proof-of-concept results using single NEX DWI. Quant Imaging Med Surg 2024;14:9533-42.
9. Yao DQ, Zheng CJ, Deng YY, Lu BL, Lu T, Hu GW, Li XM, Xiao BH, Ma FZ, Sabarudin A, King AD, Wáng YXJ. Potential diverse applications of diffusion-derived vessel density (DDVD) pixel-by-pixel mapping. Quant Imaging Med Surg 2024;14:2136-45.
10. Li XM, Yao DQ, Quan XY, Li M, Chen W, Wáng YXJ. Perfusion of hepatocellular carcinomas measured by diffusion-derived vessel density biomarker: Higher hepatocellular carcinoma perfusion than earlier intravoxel incoherent motion reports. NMR Biomed 2024;37:e5125.
11. Lu BL, Yao DQ, Wáng YXJ, Zhang ZW, Wen ZQ, Xiao BH, Yu SP. Higher perfusion of rectum carcinoma relative to tumor-free rectal wall: quantification by a new imaging biomarker diffusion-derived vessel density (DDVD). Quant Imaging Med Surg 2024;14:3264-74.
12. Wang F, Wang Y, Qi L, Liang J, Xiao BH, Zhang C, Wáng YXJ, Ye Z. High correlation between Ki-67 expression and a novel perfusion MRI biomarker diffusion-derived vessel density (DDVD) in endometrial carcinoma. Magn Reson Imaging 2025;117:110324.
13. Ju ZG, Leng XM, Xiao BH, Sun MH, Huang H, Hu GW, Zhang G, Sun JH, Zhu MSY, Guglielmi G, Wáng YXJ. Influences of the second motion probing gradient b-value and T2 relaxation time on magnetic resonance diffusion-derived 'vessel density' (DDVD) calculation: the examples of liver, spleen, and liver simple cyst. Quant Imaging Med Surg 2025;15:74-87.
14. Yao DQ. King AD, Zhang R, Xiao BH, Wong LM, Wáng YXJ. Assessing parotid gland tumor perfusion with a new imaging biomarker DDVD (diffusion-derived 'vessel density'): initial promising results. Rofo 2025. doi: 10.1055/a-2543-3305.
15. Yu WL, Xiao BH, Ma FZ, Zheng CJ, Tang SN, Wáng YXJ. Underestimation of the spleen perfusion fraction by intravoxel incoherent motion MRI. NMR Biomed 2023;36:e4987.
16. Greenway CV, Stark RD. Hepatic vascular bed. Physiol Rev 1971;51:23-65.
17. Le Bihan D, Turner R, Moonen CT, Pekar J. Imaging of diffusion and microcirculation with gradient sensitization: design, strategy, and significance. J Magn Reson Imaging 1991;1:7-28.
18. Lemke A, Laun FB, Simon D, Stieltjes B, Schad LR. An in vivo verification of the intravoxel incoherent motion effect in diffusion-weighted imaging of the abdomen. Magn Reson Med 2010;64:1580-5.
19. Führes T, Riexinger AJ, Loh M, Martin J, Wetscherek A, Kuder TA, Uder M, Hensel B, Laun FB. Echo time dependence of biexponential and triexponential intravoxel incoherent motion parameters in the liver. Magn Reson Med 2022;87:859-71.
20. Wáng YXJ. An explanation for the triphasic dependency of apparent diffusion coefficient (ADC) on T2 relaxation time: the multiple T2 compartments model. Quant Imaging Med Surg 2025. doi: 10.21037/qims-2025-195.
21. Egnell L, Jerome NP, Andreassen MMS, Bathen TF, Goa PE. Effects of echo time on IVIM quantifications of locally advanced breast cancer in clinical diffusion-weighted MRI at 3 T. NMR Biomed 2022;35:e4654.
22. Pahwa S, Liu H, Chen Y, Dastmalchian S, O'Connor G, Lu Z, Badve C, Yu A, Wright K, Chalian H, Rao S, Fu C, Vallines I, Griswold M, Seiberlich N, Zeng M, Gulani V. Quantitative perfusion imaging of neoplastic liver lesions: A multi-institution study. Sci Rep 2018;8:4990.
23. Ippolito D, Capraro C, Casiraghi A, Cestari C, Sironi S. Quantitative assessment of tumour associated neovascularisation in patients with liver cirrhosis and hepatocellular carcinoma: role of dynamic-CT perfusion imaging. Eur Radiol 2012;22:803-11.
24. Sahani DV, Holalkere NS, Mueller PR, Zhu AX. Advanced hepatocellular carcinoma: CT perfusion of liver and tumor tissue--initial experience. Radiology 2007;243:736-43.
25. Lewin M, Laurent-Bellue A, Desterke C, Radu A, Feghali JA, Farah J, Agostini H, Nault JC, Vibert E, Guettier

C. Evaluation of perfusion CT and dual-energy CT for predicting microvascular invasion of hepatocellular carcinoma. Abdom Radiol (NY) 2022;47:2115-27.
26. Mulé S, Pigneur F, Quelever R, Tenenhaus A, Baranes L, Richard P, Tacher V, Herin E, Pasquier H, Ronot M, Rahmouni A, Vilgrain V, Luciani A. Can dual-energy CT replace perfusion CT for the functional evaluation of advanced hepatocellular carcinoma? Eur Radiol 2018;28:1977-85.
27. Ganga KP, Gupta P, Kalra N, Behra A, Kapoor R, Duseja A, Chawla Y, Sandhu MS. Role of Computed Tomography Perfusion in Patients with Liver Cirrhosis and Hepatocellular Carcinoma. J Clin Exp Hepatol 2024;14:101259.
28. Sacco R, Faggioni L, Bargellini I, Ginanni B, Battaglia V, Romano A, Bertini M, Bresci G, Bartolozzi C. Assessment of response to sorafenib in advanced hepatocellular carcinoma using perfusion computed tomography: results of a pilot study. Dig Liver Dis 2013;45:776-81.
29. Wang S, Li B, Li P, Xie R, Wang Q, Shi H, He J. Feasibility of perfusion and early-uptake (18)F-FDG PET/CT in primary hepatocellular carcinoma: a dual-input dual-compartment uptake model. Jpn J Radiol 2021;39:1086-96.
30. Li JP, Zhao DL, Jiang HJ, Huang YH, Li DQ, Wan Y, Liu XD, Wang JE. Assessment of tumor vascularization with functional computed tomography perfusion imaging in patients with cirrhotic liver disease. Hepatobiliary Pancreat Dis Int 2011;10:43-9.
31. Li XR, Ou SX, Peng GM, Qian M. Comparative Study of Dual Source CT Perfusion Imaging in Hepatocellular Carcinoma, Hepatic Hemangioma and Focal Nodular Hyperplasia. Chinese Journal of CT and MRI 2016;14:68-70.
32. Jerome NP, d'Arcy JA, Feiweier T, Koh DM, Leach MO, Collins DJ, Orton MR. Extended T2-IVIM model for correction of TE dependence of pseudo-diffusion volume fraction in clinical diffusion-weighted magnetic resonance imaging. Phys Med Biol 2016;61:N667-80.
33. Ma FZ, Wáng YXJ. T(2) relaxation time elongation of hepatocellular carcinoma relative to native liver tissue leads to an underestimation of perfusion fraction measured by standard intravoxel incoherent motion magnetic resonance imaging. Quant Imaging Med Surg 2024;14:1316-22.
34. Li YT, Cercueil JP, Yuan J, Chen W, Loffroy R, Wáng YX. Liver intravoxel incoherent motion (IVIM) magnetic resonance imaging: a comprehensive review of published data on normal values and applications for fibrosis and tumor evaluation. Quant Imaging Med Surg 2017;7:59-78.
35. Kim BR, Song JS, Choi EJ, Hwang SB, Hwang HP. Diffusion-Weighted Imaging of Upper Abdominal Organs Acquired with Multiple B-Value Combinations: Value of Normalization Using Spleen as the Reference Organ. Korean J Radiol 2018;19:389-96.
36. Martirosian P, Boss A, Deimling M, Kiefer B, Schraml C, Schwenzer NF, Claussen CD, Schick F. Systematic variation of off-resonance prepulses for clinical magnetization transfer contrast imaging at 0.2, 1.5, and 3.0 tesla. Invest Radiol 2008;43:16-26.
37. Piekarski J, Goldberg HI, Royal SA, Axel L, Moss AA. Difference between liver and spleen CT numbers in the normal adult: its usefulness in predicting the presence of diffuse liver disease. Radiology 1980;137:727-9.
38. Wáng YXJ, Ma FZ. A tri-phasic relationship between T2 relaxation time and magnetic resonance imaging (MRI)-derived apparent diffusion coefficient (ADC). Quant Imaging Med Surg 2023;13:8873-80.
39. Wáng YXJ, Aparisi Gómez MP, Ruiz Santiago F, Bazzocchi A. The relevance of T2 relaxation time in interpreting MRI apparent diffusion coefficient (ADC) map for musculoskeletal structures. Quant Imaging Med Surg 2023;13:7657-66.

Cite this article as: Wáng YXJ, Li CY, Yao DQ, Tang SN, Xiao BH. The impacts of time of echo (TE) and time of repetition (TR) on diffusion-derived 'vessel density' (DDVD) measurement: examples of liver, spleen, and hepatocellular carcinoma. Quant Imaging Med Surg 2025;15(4):3771-3778. doi: 10.21037/qims-2025-270

